Broadband all-order polarization mode dispersion compensation via wavelength-by-wavelength Jones matrix correction

Houxun Miao,[1,*] Andrew M. Weiner,[1] Leo Mirkin,[2] and Peter J. Miller[2]

[1]*Purdue University, West Lafayette, Indiana 47907, USA*
[2]*CRI Inc., Woburn, Massachusetts 01801, USA*
**Corresponding author: hmiao@purdue.edu*

Received May 16, 2007; revised July 5, 2007; accepted July 6, 2007;
posted July 11, 2007 (Doc. ID 83154); published August 2, 2007

We demonstrate wideband all-order polarization mode dispersion (PMD) compensation by applying high-speed spectral polarization sensing and ultrafast pulse shaping techniques to characterize and correct the frequency-dependent Jones matrix associated with PMD of optical fibers on a wavelength-by-wavelength basis. We report full compensation of ~800 fs pulses distorted to more than 10 ps by a PMD module with ~5.5 ps mean differential group delay. The sensing and compensation of Jones matrix take ~200 and ~500 ms, respectively. © 2007 Optical Society of America

OCIS codes: 060.2330, 260.5430, 320.5540.

As the bit rates and distance continue to increase, polarization mode dispersion (PMD) has emerged as a key factor limiting high-speed transmission in optical fiber links [1]. Most of the current PMD compensation work is restricted to the low-order (first- and second-order) PMD approximation [2,3]. However, as the bandwidth of telecommunication systems increases, all-order PMD effects become increasingly important [4]. In our group's previous work [5], we demonstrated for what is believed to be the first time experimental wideband all-order PMD compensation by first rotating the distorted frequency-dependent state of polarization (SOP) spectra to a fixed state and then characterizing and correcting the phase of the resulting spectrum. The performance of the compensator is mainly limited by the phase measurement process, which takes several minutes. Furthermore, the measurement accuracy depends strongly on the complexity of the distorted pulses. As a result the algorithm does not work well when the mean differential group delay (DGD) exceeds ~2 times the input pulse width and lacks the robustness that will be needed for real applications.

In this Letter, we introduce a new method for all-order PMD compensation based on wavelength-parallel characterization and compensation of the frequency-dependent Jones matrix associated with PMD. We demonstrate all-order compensation of ~800 fs pulses distorted and spread to as much as 10 ps in duration, as a result of PMD with 5.5 ps mean DGD. Importantly, our new scheme derives all required phase information directly from the polarimetry data, which opens the door to robust real-time sensing and control. With current hardware, the frequency-dependent Jones matrix characterization process takes ~200 ms (can be improved to <20 ms) and the compensation process takes ~500 ms (limited by the control electronics) for each PMD compensation trial. The potential response time of our PMD compensation technique will be under 1 s after the sensing and compensation systems are automated.

In the absence of polarization dependent loss (PDL) and polarization dependent gain (PDG), the Jones matrix of a fiber link (isotropic chromatic dispersion term excluded) can be written in the Caley–Klein form [6] as

$$U_f = \begin{bmatrix} \cos\theta e^{j\phi} & \sin\theta e^{j\psi} \\ -\sin\theta e^{-j\psi} & \cos\theta e^{-j\phi} \end{bmatrix},$$

where θ, ϕ, and ψ are frequency-dependent angles. By measuring the output SOPs of 0° linear and 45° linear input SOPs, one can solve θ, ϕ, and ψ analytically. Since PMD is related to the frequency dependence of the Jones matrix, all-order PMD compensation can be achieved by correcting the Jones matrix to a constant, frequency-independent matrix. To characterize the frequency dependence of the Jones matrix, we sequentially transform the arbitrary input SOP to four different SOPs, launch them into the fiber link, and measure the output SOPs using our fast wavelength-parallel polarimeter technology [7]. Then we select the two output SOP spectra whose relative angle is closest to 90° on the Poincaré sphere. By associating one of the selected output SOP spectra with the 0° linear input SOP, and the normalized cross product of the two selected output SOPs with the 45° linear input SOP, one gets the frequency-dependent Jones matrix $U_f' = U_f U$, where U is a frequency-independent matrix and U^{-1} transforms one of the selected input SOPs to 0° linear state and the normalized cross product of the two selected input SOPs to 45° linear states. Note, it is necessary to make sure the angle between the two selected SOPs is close to 90° to avoid enlarging errors through the cross produce operation. The inverse of U_f',

$$U_f' = \begin{bmatrix} \cos\theta' e^{j\phi'} & \sin\theta' e^{j\psi'} \\ -\sin\theta' e^{-j\psi'} & \cos\theta' e^{-j\phi'} \end{bmatrix},$$

can be written as the product of three elementary rotation matrices,

$$(U_f')^{-1} = \begin{bmatrix} \exp(-j\theta_3) & 0 \\ 0 & \exp(j\theta_3) \end{bmatrix} \times \begin{bmatrix} \cos\theta_2 & -j\sin\theta_2 \\ -j\sin\theta_2 & \cos\theta_2 \end{bmatrix} \times \begin{bmatrix} \exp(-j\theta_1) & 0 \\ 0 & \exp(j\theta_1) \end{bmatrix}, \quad (1)$$

where, $\theta_1 = (\phi' + \psi')/2 + \pi/4$, $\theta_2 = -\theta'$, and $\theta_3 = (\phi' - \psi')/2 - \pi/4$ and each of these angles is frequency dependent. To achieve wavelength-by-wavelength Jones matrix correction, we disperse different optical frequency components spatially in a pulse shaping configuration [8]. We use a novel four-layer liquid crystal modulator (LCM) array to realize the three elementary rotation matrices. Each LCM layer functions as a linear retarder array (128 pixels) with fixed fast axis and arbitrarily adjustable retardance. The orientations of the four LCM layers are 0°, 45°, 0°, and 90°. We operate the first three layers (0°, 45°, 0°) to produce the three elementary rotation matrices on the right side of Eq. (1). After that operation, an isotropic spectral phase of $-(\theta_1 + \theta_2 + \theta_3)$ remains. Therefore, we program the third and fourth LCM layers in common mode to remove the unwanted remaining isotropic phase. The third LCM layer then is programmed according to the superposition of this isotropic phase and the appropriate rotation matrix from Eq. (1). After such a Jones matrix correction, PMD effects are compensated to all order. The output Jones vector after PMD compensation is a frequency-independent transformation of the input Jones vector, $\vec{E}_{\text{out}} = U^{-1}\vec{E}_{\text{in}}$.

Figure 1 shows our experimental setup. A passively mode-locked fiber ring laser followed by a bandpass filter (~4 nm FWHM) is used to produce ~800 fs pulses with 50 MHz repetition rate and 1550 nm center wavelength. We use two ferroelectric liquid crystal (FLC) retarders to switch the input SOP among four states. (Note, we do not need to know the input SOP prior to the FLCs, as long as it is constant during each measurement cycle of ~200 ms, which should be easy to achieve at the transmitter.) Each FLC acts as a quarter-wave retarder at 1550 nm and has two stable optic-axis orientations separated by approximately 45°. The switching time between axes is ~70 μs. The orientations of the axes of the two FLCs are 0° (state 0)–45° (state 1) and 45° (state 0)–90° (state 1), respectively. Consequently, the SOP transformations are denoted by the combination of the FLC states as 00, 01, 10, 11. Simulation shows that for any input SOP, there are at least two FLC states yielding output SOPs separated by an angle in the range between 60° and 120° on the Poincaré sphere. This guarantees that the Jones matrix char-

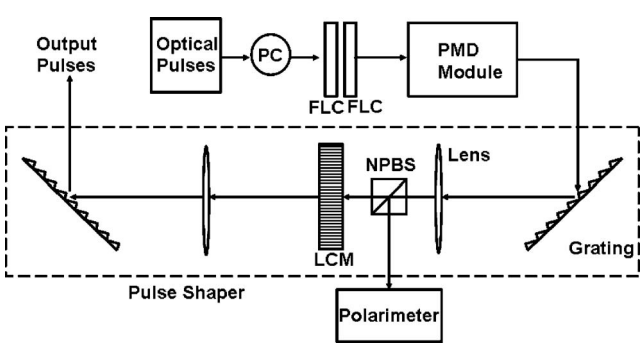

Fig. 1. Experimental setup. PC, polarization controller; FLC, ferroelectric liquid crystal; NPBS, nonpolarizing beam splitter; LCM, liquid crystal modulator.

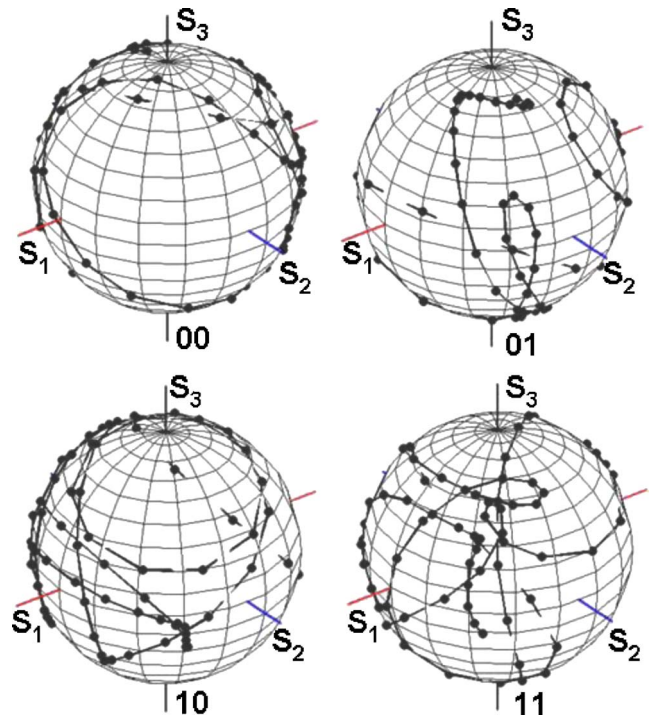

Fig. 2. (Color online) Output SOP spectra corresponding to the 4 FLC states 00, 01, 10, and 11. The spectrum range is 1545.5–1554.7 nm. Each point corresponds to a measured SOP vector at a specified wavelength, SOPs of adjacent wavelength are connected via solid lines.

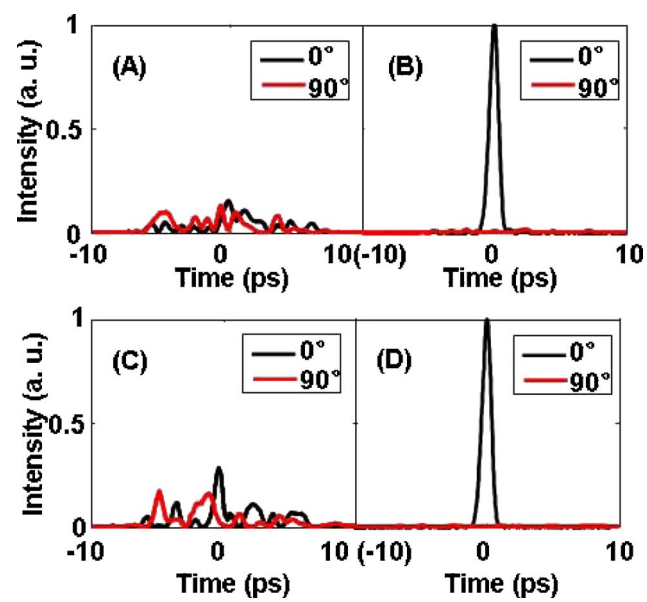

Fig. 3. (Color online) (A) and (B) Distorted and restored pulses when 00–01 states are selected for PMD compensation. (C) and (D) Distorted and restored pulses when 10–11 states are selected for PMD compensation.

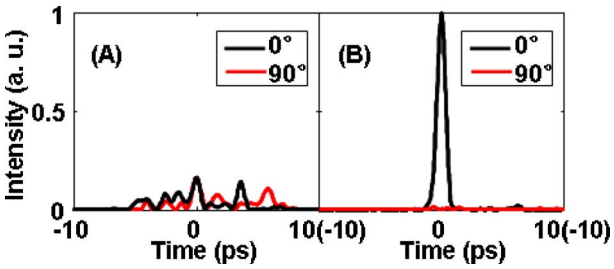

Fig. 4. (Color online) Distorted and restored pulses.

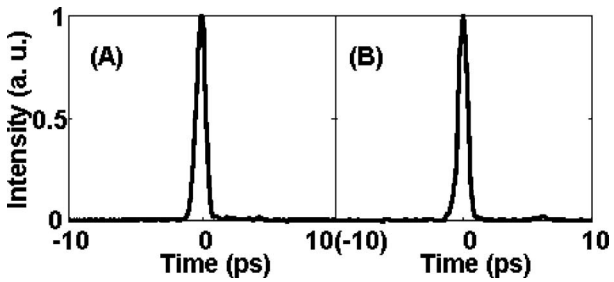

Fig. 5. Restored pulses corresponding to Figs. 3(b) and 4(b), measured with polarization insensitive cross correlation while FLCs kept switching.

acterization will be accurate enough. The pulses are then launched into a PMD module consisting of three homemade PMD emulators connected via polarization controllers (PCs). The estimated overall mean DGD is ~5.5 ps. The output light is connected to a fiber pigtailed pulse shaper incorporating the four-layer LCM. A nonpolarizing beam splitter directs a fraction of the light to the wavelength-parallel polarimeter for SOP sensing. Temporal profiles of pulses before and after PMD compensation are measured via intensity cross correlation. The chromatic dispersion of the whole setup is precompensated.

Figure 2 shows an example of four Poincaré sphere plots (corresponding to the four FLC states) of SOP spectra distorted by PMD. The strong and irregular variation of the output SOPs with wavelength is indicative of significant all-order PMD effects. The average angles between states 00–01, 00–10, 00–11, 01–10, 01–11, and 10–11 are 89.2°, 107.9°, 107.2°, 159.4°, 108.9°, and 59.0°. We first select the data from 00–01 states for control of our PMD compensator. Since PMD distorted pulses are polarization dependent, we measure the temporal intensity profiles at two orthogonal polarization states (0° and 90° linear) selected by a polarizer. For now we keep the FLC retarders stable (00 state) during the measurement. Figures 3(a) and 3(b) show the PMD distorted pulses and the restored pulses after PMD compensation. The peak intensity of the restored pulse at 0° linear SOP is normalized to 1. After compensation, the pulse is compressed dramatically from more than 10 ps (10% intensity) to 826 fs (FWHM). The output SOP of state 00 is corrected to 0° linear state as predicted in theory. To demonstrate the robustness of our PMD sensing–compensation system, we now repeat the experiment with identical PMD but using the data from the 10–11 FLC sensing states (the angle between which is even out of the 60°–120° range). We keep the FLC retarders on the 10 state during the cross-correlation measurement. Figures 3(c) and 3(d) show results. Again the pulse is compressed to 811 fs. By adjusting the PC before the FLCs and the PCs between the PMD emulators, we then repeated the experiments with more than 20 independent PMD profiles and input SOPs. Each time, we can compress the pulses to a comparable ~800 fs duration after PMD compensation. Figure 4 shows the results from one of these additional trials. The pulse is compressed to 828 fs.

Our PMD compensation technique is compatible with simultaneous real-time sensing and compensation. To demonstrate this, we measured the intensity profiles of the restored pulses while keeping the sensing FLC retarders switching at a rate of ~20 Hz during the experimental trials of Figs. 3 and 4. The slow polarization switching will degrade the cross-correlation measurement because the second harmonic nonlinearity is strongly polarization dependent. Here we employed a novel polarization insensitive cross-correlation technique to average out the polarization switching induced measurement degradation, where the SOP after PMD compensation is scrambled at a rate of 700 KHz, which is much faster than the measurement integration time [9]. Figures 5(a) and 5(b) show the restored pulses corresponding to Figs. 3(b) and 4(b), respectively. The measured pulse FHWMs are 811 and 823 fs, respectively, confirming that the PMD compensation process is insensitive to changes in input SOP.

In conclusion, we demonstrated all-order compensation of ~800 fs pulses distorted by PMD with ~5.5 ps mean DGD. Compared to our previous work, we have improved the compensated mean DGD more than threefold and the response speed by more than 2 orders of magnitude.

The authors thank S. X. Wang, L. Xu, Z. Jiang, and D. E. Leaird for their contributions. This work was funded in part by the National Science Foundation under grant 0501366-ECS.

References

1. H. Kogelnik, R. M. Jopson, and L. E. Nelson, in *Optical Fiber Telecommunications IVB-Systems and Impairments*, I. P. Kaminow and T. Li, eds. (Academic, 2002), p. 723.
2. Q. Yu, L.-S. Yan, Y. Xie, M. Hauer, and A. E. Willner, IEEE Photon. Technol. Lett. **13**, 863 (2001).
3. P. B. Phua and H. A. Haus, IEEE Photon. Technol. Lett. **14**, 1270 (2002).
4. M. Shtaif and M. Boroditsky, IEEE Photon. Technol. Lett. **15**, 1369 (2003).
5. M. Akbulut, A. M. Weiner, and P. J. Miller, Opt. Lett. **30**, 2691 (2005).
6. J. P. Gordon and H. Kogelnik, Proc. Natl. Acad. Sci. U.S.A. **97**, 4541 (2000).
7. S. X. Wang and A. M. Weiner, J. Lightwave Technol. **24**, 3982 (2006).
8. A. M. Weiner, Rev. Sci. Instrum. **71**, 1929 (2000).
9. H. Miao, A. M. Weiner, C. Langrock, R. V. Roussev, and M. M. Fejer, Opt. Lett. **32**, 874 (2007).